


| | | | |
|---|---|------------|---|
|  | SAKARYA ÜNİVERSİTESİ FEN BİLİMLERİ ENSTİTÜSÜ DERGİSİ <i>SAKARYA UNIVERSITY JOURNAL OF SCIENCE</i> | |  |
| | e-ISSN: 2147-835X Dergi sayfası: http://www.saujs.sakarya.edu.tr | | |
| | <u>Geliş/Received</u> <u>Kabul/Accepted</u> | <u>Doi</u> | |

NONLINEAR FINITE ELEMENT ANALYSIS OF INTERVERTEBRAL DISC: A COMPARATIVE STUDY

Suzan Cansel Dogru*¹

ABSTRACT

The aims of this study are *i)* to build up finite element model of the functional spinal unit without ligaments from cervical region, and *ii)* to compare the effects of mildly, moderately and severely level degenerated intervertebral disc on the stress during flexion, lateral bending, and rotation. For this, the three-dimensional vertebral model was build up as a three-layered structure with different material properties, from a two-dimensional computed tomography image taken from a subject. The disc was defined by hyperelastic material properties. C3 vertebra is fixed from its inferior endplate at 6 axes movements. 50 N axial compression force was applied to superior endplate of the C2 vertebrae. 1 Nm of flexion, lateral bending and rotation moments were applied to superior endplate of the C2 vertebra. The von Mises stress on the annulus and nucleus for healthy and different level degenerated intervertebral disc were calculated for the different direction of movements by finite element analysis. The results showed that the effect of flexion moment increased the stress in the annulus more than the other moment directions as the degeneration progressed. While the stress in the nucleus decreased during flexion as degeneration progressed, the stress either remained the same or decreased by a small percentage (6%) under lateral bending and rotation moment except for rotation of the model with the severely degenerated intervertebral disc.

Keywords: Finite element analysis, intervertebral disc, 3D modelling from computed tomography.

OMURLAR ARASI DİSKİN DOĞRUSAL OLMAYAN SONLU ELEMANLAR ANALİZİ: KARŞILAŞTIRMALI ÇALIŞMA

ÖZ

Bu çalışmanın amaçları, *i)* servikal bölgeye ait bağ dokusu içermeyen fonksiyonel omurga ünitesinin sonlu elemanlar modelini geliştirmek ve *ii)* fleksiyon, yana eğilme ve rotasyon sırasında omurlar arası diskte hafif, orta ve yüksek seviyedeki dejenerasyonun gerilmeye etkilerini karşılaştırmaktır. Bunun için, denekten alınan iki boyutlu bilgisayarlı tomografi görüntüsünden, farklı malzeme özelliğine sahip üç katmanlı yapı olarak üç boyutlu omur modeli oluşturulmuştur. Disk hiperelastik malzeme özellikleri ile

* Corresponding Author

¹ Department of Mechanical Engineering, Faculty of Engineering, Istanbul University, Avcılar, Istanbul, Turkey. cansel.gurcan@istanbul.edu.tr

tanımlanmıştır. C3 omurunun alttaki son plağından 6 ekseninde hareketi sabitlemiştir. 50 N aksiyel kompresyon kuvveti C2 omurunun üstteki son plağına uygulanmıştır. 1 Nm fleksiyon, yana eğilme ve rotasyon momentleri C2 omurunun üstteki son plağına uygulanmıştır. Sağlıklı ve farklı dejenerasyon derecelerine sahip omurlar arası disklerde annulus ve nukleus üzerindeki von Mises gerilmesi sonlu elemanlar analizi ile farklı hareket yönleri için hesaplanmıştır. Sonuçlar göstermiştir ki dejenerasyon ilerledikçe fleksiyon momentinin etkisiyle annulusdaki gerilmenin artması diğer moment yönlerine göre daha fazladır. Fleksiyon sırasında dejenerasyon ilerledikçe nukleusdaki gerilme azalırken, yüksek seviyedeki omurlar arası disk dejenerasyonuna sahip modelin rotasyon sırasındaki hareketi dışında, yana eğilme ve rotasyon momenti sırasında gerilme aynı kalmış veya küçük bir oran ile (% 6) azalmıştır.

Anahtar Kelimeler: Sonlu elemanlar analizi, omurlar arası disk, bilgisayarlı tomografi ile üç boyutlu modelleme.

1. INTRODUCTION

Intervertebral disc (IVD) degeneration, common spinal disorder, has researched especially lumbar IVD degeneration in many aspects to understand reason and affects to spine. Because the IVD act acts as though a loading absorber, in time, fatigue and mechanical change i.e. functional failure occur by aging usually [1]. The fluid level in the nucleus reduces age by age. Although a healthy nucleus pulposus shows a hydrostatic pressure, the pressure distribution in a degenerated disc is nonuniform and direction dependent [2]. By decreasing fluid, the height of disc reduces, the number of fibers in the annulus increases, the disc becomes stiffer and the strain energy capability decrease [3].

In this study, the main goal is to compare changing stress on a disc of the cervical region by degeneration level and motion direction, computationally. Finite element analysis (FEA) was used to calculate the von Mises stress on a disc. Disc degenerations simulate by changing the bulk modulus of the nucleus and changing the nonlinear material property of the annulus disc.

The disc is investigated two parts as annulus fibrosus and nucleus pulposus. Nucleus pulposus is located in the midst of annulus. Nucleus prevents the development of stress concentrations, which could cause damage to the underlying vertebrae or to their endplates. According to Panjabi, the nucleus takes up 30-50 % of total disc volume. Nevertheless, Morris said that the nucleus takes up 50-60 % of total disc volume [4, 5, 6]. It contains high rates of fluid – gel matter. The property helps to distribute pressure evenly across the disc. The healthy nucleus is incompressible and well impact force absorber. In other words, the property is like a waterbed. External forces change the level of fluid in a nucleus at a micro rate. By increasing the load increase the pressure of disc and fluid act towards end plate. By decreasing the load decrease the pressure of disc and fluid return. The motion is like a pump mechanism [7]. The mechanism is supposed to disc for keeping alive. Although it has micro level pump mechanism, the approach as waterbed is realistic. According to the literature, the pressure of inside the nucleus is 0.1 – 0.2 MPa, approximately [5, 8].

Finite element analysis (FEA) generates differential equations and solves with a numerical approximation. The entire model into small elements connected by nodes is applied boundary

and load conditions. Whole nodes consist own differential equations and transfer the solution element to element. Material properties, load and boundary conditions, a geometry of the model, element types and quantity, properties of contact points and surfaces, and analysis method directly affect the results of the analysis. The software of FEA can calculate stress distribution over a model caused by external forces and other loading and boundary factors. The accuracy of finite element model (FEM) provides reliable results obtained from FEA. The FEM is preferred to carry out mechanical analyses for many complex biomechanical structures. Most of the biomechanical models including complicated geometries such as vertebrae and soft tissues, complex material properties or loading conditions cannot be possible to accomplish an analytical solution.

Conversion of 2D computed tomography (CT) data into 3D finite element model is the most widely used model generation method for biologic structures. Different biologic tissues absorb radiation at different levels, which cause different impressions on tomography data related to the radiodensity of the tissue. These radio density differences among anatomic structures are processed with tomography software by using 'Hounsfield Scale' (HU) which is a quantitative scale for describing radiodensity and computed tomography images are produced. Thanks to HU, different biological tissues distinguish up to their density and the elastic modulus defined by equation related to HU and elastic modulus [9].

2. METHODS

To obtain 3D finite element model, 2D CT data from the subject was used (Fig. 1A). In this way, different anatomic structures having different HU values from dicom file could be converted to 3D models separately and consequently, the more detailed anatomic model having different biologic structures was generated thanks to BONEMAT non-commercial software (Istituto Ortopedico Rizzoli, Italy). By setting threshold values, all tissues can be separated as cortical, spongius, disc, facets etc. The HU range of CT calibrated with air, i.e. -1200, and cortical bone, i.e. 2895, as linear [9]. A threshold based Hounsfield scale (range: 580-2895 HU) was used to isolate the cervical 2-3 (C2 – C3) vertebrae and exclude soft tissues. Functional spinal unit (FSU) as being the shortest segment of the spine shows the same

characteristics that underlie the biomechanics of the entire spine. In fact, the FSU without ligaments consists of two adjacent vertebrae with the respective IVD as seen in Fig. 1B.

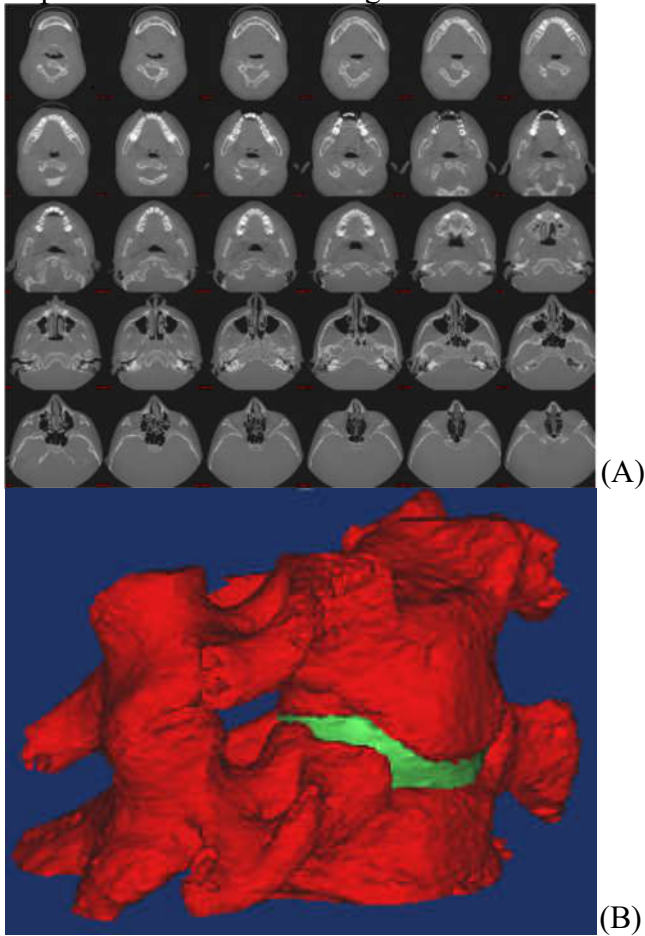


Figure 1. (A) The dicom file of CT, (B) The FSU model without ligaments.

Facet joints in each segment of the spine were simulated with 3D gap elements to transfer the force between nodes in a single direction. In each model, the same number of elements was used in each segment. For the bone meshing, 0.1 mm global edge hybrid quadratic tetrahedral element was chosen. The global edge length of 0.16 mm and quadratic tetrahedral element type was assigned to the annulus disc meshing. Entire models had 194000 elements approximately; thereby enabling the model has a high accuracy (Fig 2A).

All vertebrae were assumed to have linearly elastic-isotropic behaviour and their mechanical properties were described by Young's modulus and Poisson's ratio. The material properties were depended on the measured x-ray attenuation coefficients (Hounsfield, HU) related to density.

$$\rho = 0.44 HU + 527 \quad (1)$$

$$E = 3 * 10^{-6} * \rho^3 \quad (2)$$

The relations between HU, density and Young modulus are in formula (1) where ρ is density expressed in g/cm^3 . The formula (2) was derived

by *Gupta and Dan* [9]. E is the Young modulus expressed in N/mm^2 . As seen in the Fig. 2B, the vertebrae model was distinguished by section by section. Average HU values for all sections were measured and the Young modulus calculated from the relation e.g. blue section 9.14 GPa, green section 6.14 GPa and red section 1.94 GPa. All the poisson ratios were 0.3 [10].

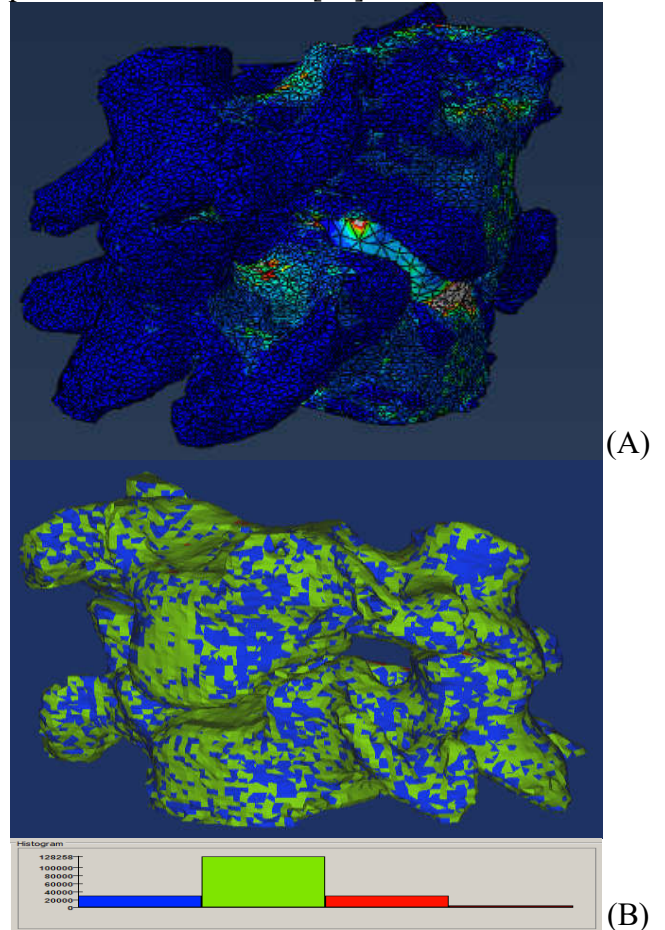


Figure 2. (A) The finite element model with stress distribution, (B) The bone model with distributed material properties.

The material property of healthy nucleus was determined as fluid-filled cavity i.e. incompressible and hydrostatic cavity. Fluid transfer of the nucleus pulposus was neglected. For the degenerated IVD, the property of compressible was simulated by bulk modulus to simulate compressible properties The bulk modulus of the nucleus was defined as 2500 MPa for the healthy nucleus, 100 MPa for mildly degenerated nucleus, 50 MPa for moderately degenerated nucleus and 20 MPa for severely degenerated nucleus [2, 11]. The periphery of the cavity was described as shell with 1 MPa Young modulus and 0.49 poisson ratio [10].

The material property of annulus fibrosus were assigned as hyperelastic material. The coefficient of Mooney-Rivlin hyperelastic material were described as $C10=0.2$, $C01=0.05$, $D1=1e^{-10}$ for

healthy annulus, $C10=0.4$, $C01=0.1$, $D1=1e^{-10}$ for mildly annulus, $C10=0.9$, $C01=0.23$, $D1=1e^{-10}$ for moderately annulus and $C10=1.8$, $C01=0.45$, $D1=1e^{-10}$ for severely annulus. All coefficients were in unit of MPa [10].

The applied loads were moment in flexion, lateral bending, and axial rotation as 1 Nm [12]. The moment was applied on superior surface of the C2 by the reference points coupled with surface portions where the adjacent vertebral body. 50 N axial compression force was applied to superior endplate of the C2 vertebrae with all moment direction. The C3 inferior surface was fixed in all direction. The contact properties with were determined to be bounded (no slip and clearance) with IVD and endplate. For all cases, the load and analysis were assumed static.

3. RESULTS

Von Mises stresses were comparatively evaluated according to the results obtained from FEA and the maximum stress over the annulus were given by Fig. 3. The maximum von Mises stresses were calculated for models with healthy, mildly degenerated, moderately degenerated and severely degenerated IVDs and given in MPa. The maximum stress was observed during flexion case.

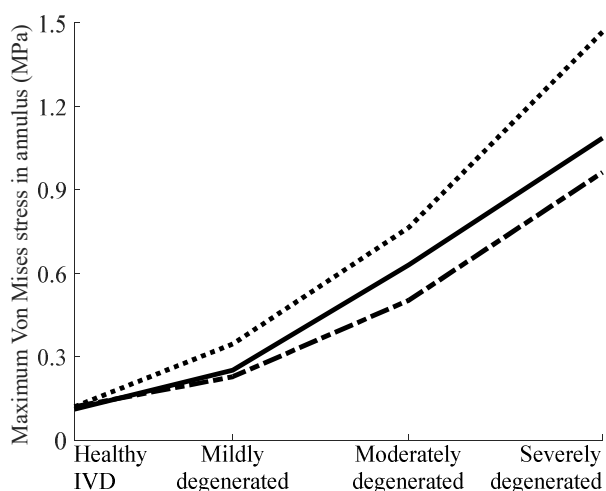


Figure 3. The maximum von Mises stress (MPa) in the annulus by healthy IVD to degenerated IVDs for flexion (dashed line), bending (dotted line) and rotation (solid line).

The maximum von Mises stress in annulus were 0.12 MPa in flexion, 0.12 MPa in lateral bending and 0.11 MPa in rotation for models with healthy IVD, 0.35 MPa in flexion, 0.23 MPa in lateral bending and 0.25 MPa in rotation for models with mildly degenerated IVD and there was no significant difference ($p>0.01$). The maximum von

Mises stress in annulus were 0.77 MPa in flexion, 0.50 MPa in lateral bending and 0.63 MPa in rotation for models with moderately degenerated IVD, 1.47 MPa in flexion, 0.97 MPa in lateral bending and 1.09 MPa in rotation for models with severely degenerated IVD and the difference with results for healthy IVD was significant ($p<0.01$). There were no significant differences between flexion, lateral bending, and rotation.

The maximum von Mises stresses over the nucleus were given by Fig. 4. The maximum von Mises stresses were calculated for models with healthy, mildly degenerated, moderately degenerated and severely degenerated IVDs and given in MPa. The maximum stress was observed during flexion case. The maximum von Mises stresses in nucleus were 0.24 MPa in flexion, 0.15 MPa in lateral bending and 0.14 MPa in rotation for models with healthy IVD, 0.21 MPa in flexion, 0.14 MPa in lateral bending and 0.14 MPa in rotation for models with mildly degenerated IVD and there was no significant difference ($p>0.01$). The maximum von Mises stresses in nucleus were 0.21 MPa in flexion, 0.14 MPa in lateral bending and 0.15 MPa in rotation for models with moderately degenerated IVD, 0.20 MPa in flexion, 0.14 MPa in lateral bending and 0.16 MPa in rotation for models with severely degenerated IVD and there was no significant difference ($p>0.01$). The differences between flexion and other directions were significant ($p<0.01$).

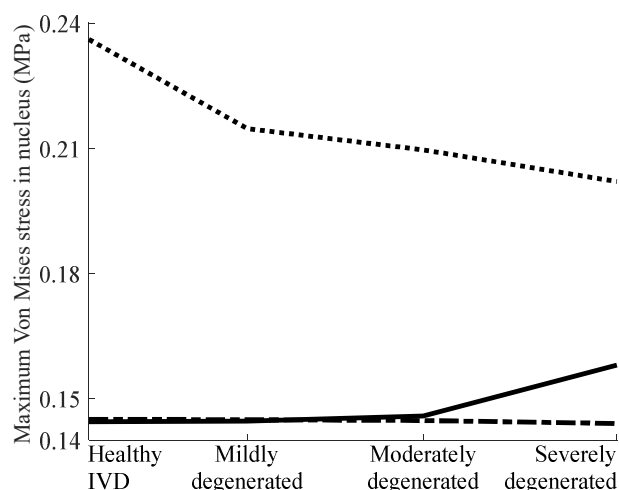


Figure 4. The maximum von Mises stress (MPa) in the nucleus of healthy and different levels degenerated IVDs for flexion (dashed line), bending (dotted line) and rotation (solid line).

During flexion moment, the height of IVD in vertical axis decreased 30% for mild to 40% for severely degenerated models rated with the healthy model.

4. CONCLUSION AND LIMITATIONS

The stress increased nearly ten-fold with the severely degenerated model for all moment directions. Though not significant, the stress in annulus under flexion moment increased more than the other directions. The results suggest that degeneration on IVD affect the spine, especially during flexion motion. The nucleus normally carries a portion of external loading and supports the annulus [13]. Due to degeneration, the nucleus cannot support the stress to external loading and as a consequence, the stress in annulus increased as the degeneration progressed. Ruberté et al. were reported that the effect of degeneration was increasing stress in the annulus and decreasing stress in the nucleus for lumbar spine [10].

Yoganandan et al. were reported that the maximum intradiscal pressure in the nucleus was the highest under combined compression and flexion and reached 0.24 MPa [14]. Their similar results can be evaluated as validation of finite element model.

The decreasing stress in the nucleus was maximum under flexion moment. Decreasing in nucleus stress was reached 20%. The results suggest that the effect of degeneration mostly occurred under flexion moment. Nucleus stress either remained the same or decreased by a small percentage (6%) under lateral bending and rotation moment except rotation in the model with severely degenerated IVD. Facets resist rotation and lateral bending moment [15]. Remaining same stress in the nucleus during lateral bending and rotation moment may be occurred due to carrying the load by facets and not affected by IVD degeneration. The result of the severely degenerated model suggests that increasing stress under rotation moment may be the consequence of degeneration in facet joints.

The height of IVD reduced as the degeneration progressed. Adams and Roughley were reported that increasing stress cause the decreasing height of IVD as the degeneration progressed [16]. The stress values of degenerated IVD obtained with bulk modulus were increased. The results suggest that the fluid-filled cavity with bulk modulus provide realistic results for simulating the degenerated IVD.

A lot limitation was existence in the study. To develop the model at axial rotation and lateral bending, the material properties of facets should be described as nonlinear. The ligaments should be added in the model because of resisting property.

The dynamic analysis should be used due to changing the results as more realistic. In addition, the annulus disc model should have ground substance and fibers. The material properties of bone should be dependent on time and loading condition. By increasing the load on a bone, the bone will be stronger i.e. remodel itself expressed as Wolff's law. The model obtained from CT, cannot simulate with an effect of Wolff's law. The elastic modulus obtains from HU value. The value is a quantitative scale for describing radiodensity. It is valid for static analysis with elastic materials. The analysis should solve with dynamic case e.g. bone remodelling (Wolff's law) and osteoporosis. Time depended material properties cannot obtain and the analysis cannot reflect the truth [17].

REFERENCES

- [1] J. Miller, C. Schmatz, and A. Schultz, "Lumbar disc degeneration: correlation with age, sex, and spine level in 600 autopsy specimens," *Spine*, vol. 13, pp. 173–178, 1988.
- [2] A. Rohlmann, T. Zander, H. Schmidt, H. J. Wilke, and G. Bergmann, "Analysis of the influence of disc degeneration on the mechanical behaviour of a lumbar motion segment using the finite element method," *J. Biomech*, vol. 39, pp. 2484-2490, 2006.
- [3] R. Gunzburg, R. Parkinson, R. Moore, F. Cantraine, W. Hutton, B. Vernon-Roberts, and R. Fraser, "A cadaveric study comparing discography, magnetic resonance imaging, histology, and mechanical behavior of the human lumbar disc," *Spine*, vol. 17, pp. 417–426, 1992.
- [4] M. Panjabi, and A. A. White, *Clinical Biomechanics of the Spine*, Lippincott-Raven Publications, Philadelphia, New York, 1990.
- [5] A. Nachemson and J. M. Morris, "In vivo measurements of intradiscal pressure discometry, a method for the determination of pressure in the lower lumbar discs," *J Bone Joint Surg*, vol. 46, pp. 1077-1092, 1964.
- [6] J. M. Morris and et al., "The structural components of the IVD," *J Bone Joint Surg*, vol. 56, pp. 4, 1974.
- [7] A. B. Joshi, "Mechanical behavior of the human lumbar intervertebral disc with polymeric hydrogel nucleus implant: an experimental and finite element study," doctorate thesis, Drexel University, 2004.
- [8] H. J. Wilke, and et al., "New in vivo measurements of pressures in the intervertebral

- disc in daily life,” *Spine*, Vol. 24, pp. 755-762, 1999.
- [9] S. Gupta and P. Dan, “Bone geometry and mechanical properties of the human scapula using computed tomography data,” *Trends Biomater Artif Organs*, vol. 17, pp. 61-70, 2004.
- [10] L. M. Ruberté, R. N. Natarajan, and G. B. Andersson, “Influence of single-level lumbar degenerative disc disease on the behavior of the adjacent segments—a finite element model study,” *J Biomech*, vol. 42, 341-348, 2009.
- [11] T. Mustafy, M. El-Rich, W. Mesfar, and K. Moglo, “Investigation of impact loading rate effects on the ligamentous cervical spinal load-partitioning using finite element model of functional spinal unit C2–C3,” *J Biomech*, vol. 47, pp. 2891-2903, 2014.
- [12] A. P. del Palomar, B. Calvo, and M. Doblare, “An accurate finite element model of the cervical spine under quasi-static loading,” *J Biomech*, vol. 41, pp. 523-531, 2008.
- [13] A. Shirazi–adl, “Finite-element simulation of changes in the fluid content of human lumbar discs: mechanical and clinical implications,” *Spine*, vol. 17, pp. 206-212, 1992.
- [14] N. Yoganandan, S. Kumaresan, and F. A. Pintar, “Biomechanics of the cervical spine Part 2. Cervical spine soft tissue responses and biomechanical modeling,” *Clinical biomech*, vol. 16, pp. 1-27, 2001.
- [15] M. Kurutz, “Finite element modelling of human lumbar spine,” In *Finite Element Analysis*. Sciyo, 2010.
- [16] M. A. Adams, and P. J. Roughley, “What is intervertebral disc degeneration, and what causes it?” *Spine*, vol. 31, pp. 2151-2161, 2006.
- [17] S.C. Cowin, “Wolff’s law of trabecular architecture at remodeling equilibrium,” *J Biomech Eng*, vol. 108, pp. 83-88, 1986.